

DOI: 10.1070/QEL16108

Scattering of a laser beam on a wet blood smear and measurement of red cell size distribution

Yu.S. Yurchuk, V.D. Ustinov, S.Yu. Nikitin, A.V. Priezzhev

Abstract. **We report an automated laser system that allows the red cell size distribution to be measured. Experiments are performed on laser light scattering by a suspension of oriented red blood cells (a wet blood smear). Based on an analysis of the angular distribution of light intensity in the diffraction pattern, we have restored the red cell size distribution. The average diameter of a red blood cell is determined with an error of less than 1%, and the spread of red blood cells in size – with an error of about 20%. We discuss the problems of photometry and processing of diffraction patterns, preparing blood samples and data processing algorithms, including methods for solving the inverse scattering problem.**

Keywords: *wet blood smear, laser diffraction, the distribution of red blood cells in size.*

1. Introduction

A distribution curve of measured diameters of red blood cells (the Price-Jones curve) is an important rheological characteristic of blood. Standard blood tests measure the basic parameters of this distribution, i.e., mean cell volume (MCV) and red cell distribution width (RDW). Normally, the average volume of red blood cells is about 90 μm^3, and the red cell distribution width is 12%–14%. An increased distribution width leads to the risk of cardiovascular and other diseases [1]. This parameter can be approximately assessed by visual microscopic examination of a blood smear. A more accurate measurement is possible by using automated smear-image analysis performed by a computer [2]. However, both methods are complicated in practical implementation and require much computation time.

Modern automatic blood analysers plot a red cell size distribution curve using electrical (Coulter counter [3]) or optical (flow cytometry) techniques [4]. In both cases, the measurement is performed on individual cells (about 10000). These measurements are also very time-consuming or require expensive equipment. Another method of measurements is based on laser diffractometry. In this case, the size distribution of red blood cells is found by analysing the diffraction pattern emerging in the scattering of a laser beam on erythrocytes. In principle, such measurements are possible on dry blood smears [5, 6] or suspensions of erythrocytes [7, 8]. However, their practical implementation requires a number of problems to be solved, such as preparation of high-quality blood smears, photometry of diffraction patterns, suppression of the speckle noise of diffraction patterns, and development of special data processing algorithms. In this context, increased importance is attached to the development of theoretical models. We have developed an analytical model of scattering of a laser beam on an inhomogeneous ensemble of particles mimicking red blood cells [9]. Using this model, we have found an approximate relation between the dispersion of particle sizes and the diffraction pattern visibility [10]. More accurate models are based on the use of modern numerical techniques such as discrete dipole approximation [11], boundary element method [12], method of integral equations [13], etc.

Using a phase microscope, Lim et al. [14] studied the shape of red blood cells in a dry blood smear. The data obtained show that the shape of erythrocytes in these conditions significantly differs from that of a biconcave disc, which a red blood cell has in a liquid medium. In this connection, we used a thin layer of red blood cell suspension (wet blood smear). We prepared this smear by placing a dilute suspension of red blood cells between two panes of glass separated by a distance of approximately 100 μm. According to our observations, in the case of the horizontal arrangement of the smear, red blood cells settle to the bottom of the cell and are oriented parallel to the surface of the glass. Thus, the wet swab combines the advantages of a dry smear (orientation of red blood cells) and suspension (preservation of the natural shape of the cells). We note one more important fact: In a wet blood smear, a jump in the refractive index at the surface of erythrocytes is much lower than that in the case of a dry smear. This makes it possible to consider red blood cells in a liquid as optically soft particles. An erythrocyte, which is in a liquid, can be simulated by a flat transparent disc, and the accuracy of this approximation is quite high [15], which greatly simplifies the theoretical model and the analysis of the experimental data. In this paper we consider the possibility of measuring the red cell size distribution on a wet smear of blood by means of laser diffractometry.

2. Theoretical model

In the experiments we use the radiation from a helium–neon laser with a wavelength of 633 nm. At this wavelength, red blood cells weakly absorb light and, therefore, we will consider them to be transparent particles. A normal erythrocyte is a biconcave disc with an average diameter of about 7.5 μm, a thickness of about 1 μm in the centre and an edge thickness

Yu.S. Yurchuk, V.D. Ustinov, S.Yu. Nikitin, A.V. Priezzhev Faculty of Physics and International Laser Center, M.V. Lomonosov Moscow State University, Vorob'evy gory, 119991 Moscow, Russia; e-mail: sergeynikitin007@yandex.ru

Received 21 April 2016
Kvantovaya Elektronika **46** (6) 515–520 (2016)
Translated by I.A. Ulitkin

of about 2 μm. Red blood cells are placed in a liquid medium, where their relative refractive index is 1.05. For the analysis we will use a part of the diffraction pattern, which lies outside the direct laser beam and contains first- and second-order intensity minima. This is a region of scattering angles from 1 to 10°. As shown in [15], in these conditions, scattering of light by an erythrocyte scarcely differs from scattering by a flat disc of the same size.

Let us consider the diffraction of a laser beam on a blood smear. We consider erythrocytes to be transparent flat discs and assume that all cells lie in the same plane, perpendicular to the laser beam. To take into account the variation of red blood cells in size, we assume the radius of an erythrocyte to be a discrete random variable with the distribution function $p_j(R_j)$. For simplicity, we set $R_j = \bar{R} + jr$, where $\bar{R}$ is the average value of the red blood cell radius; r is the step of the radius variation; and $j = 0, \pm1, \pm2, \ldots, \pm m$. The objective is to find the size distribution of red blood cells, based on the analysis of the diffraction pattern emerging in the scattering of the laser beam by the blood smear.

In the anomalous diffraction approximation [16], the light scattering by a transparent flat plate is equivalent to the diffraction of a plane light wave at an opening of the same shape [9, 17]. In particular, scattering by a transparent circular disc in the far-field diffraction region is described by the formula [18, 19]

$$I(\theta) = I_0 |\gamma|^2 \left(\frac{\pi R^2}{\lambda z}\right)^2 \left[\frac{J_1(2\pi R\theta/\lambda)}{\pi R\theta/\lambda}\right]^2. \quad (1)$$

Here, $J_1(x)$ is the Bessel function of the first kind; I is the intensity of light; θ is the scattering angle; I_0 is the laser radiation intensity; R is the radius of the plate; λ is the wavelength of light; z is the distance from the plate to the observation screen; $\gamma = \exp(-i\Delta\varphi) - 1$ is the parameter depending on the plate material and its thickness h; $\Delta\varphi = kn_0h(m - 1)$ is the phase shift of rays passing through a particle as compared with the phase shift of rays that have passed by it; $k = 2\pi/\lambda$ is the wavenumber; m is the relative refractive index of the plate; and n_0 is the absolute refractive index of the surrounding medium.

Note that this model is one of the fundamental in the theory of scattering of light by red blood cells (see, for example, [5]). It is called the 'shadow cross-section model' [20]. The experimental substantiation of this model relies on the similarity of the scattering pattern of the laser beam by a blood smear with the diffraction pattern of a plane light wave by a circular aperture (see, for example, [17, 21]). The advantage of this model is that it allows one to analytically describe light scattering by an ensemble of red blood cells, which is important for the development of data processing algorithms. In particular, this model helped to find approximate expressions for the mean radius $\bar{R}$ and the scatter of red blood cells in their size $\delta_R = \langle(R/\bar{R} - 1)^2\rangle^{1/2}$ on a blood smear [10, 17]. These expressions have the form:

$$\bar{R} = 0.61\lambda/\theta_1,\ \delta_R = \sqrt{(1 - v)/76}\,.$$

Here, θ_1 is the angle at which the first minimum in the diffraction pattern is observed; $v = (I_2 - I_1)/(I_2 + I_1)$ is the visibility of a specific portion of the diffraction pattern; and I_1 and I_2 are the intensities of the first minimum and first maximum in the diffraction pattern, respectively.

In scattering of a laser beam by a single erythrocyte, the Fraunhofer diffraction zone begins at a distance of $z_d = kd^2/2 = 0.3$ mm from the red blood cell (d is the diameter of a red blood cell). However, we need the first minimum of the diffraction pattern to extend beyond the direct laser beam. At a beam diameter $D = 2$ mm, this occurs at a distance $z = Dd/2.44\lambda \approx 1$ cm from the blood smear. Therefore, the observation screen should be place at a distance of no less than 1 cm from the smear. This condition was satisfied in our experiments.

Using the theoretical model developed in [9, 10, 17], we can write the normalised angular distribution of the intensity of light scattered by a blood smear:

$$F(\theta) = \beta \sum_j p_j \left(\frac{\pi R_j^2}{\lambda z}\right)^2 \left[\frac{J_1(2\pi R_j\theta/\lambda)}{\pi R_j\theta/\lambda}\right]^2 + \Phi, \quad (2)$$

where z is the distance from the blood smear to the observation screen. Parameters β and Φ are the constant dimensionless quantities. The first of them allows one to write the intensity distribution in arbitrary units (which is useful for comparison of the theory with the experiment), and the second takes into account the existence of a background in the diffraction pattern. This background is caused by noises of different nature, random orientation of part of the red blood cells in space, etc.

Equation (2) was obtained under the following assumptions: The observation screen is located in the far-field diffraction zone; all cells have the same thickness; cells on the smear are located randomly; and the diffraction pattern is averaged over random coordinates of cells, providing a suppression of the speckle noise of the diffraction pattern.

Equation (2) gives the solution of the direct problem of diffraction, i.e., expresses the light intensity distribution in the diffraction pattern through the characteristics of an ensemble of particles. To solve the inverse problem, i.e., to find the red cell size distribution with the help of laser diffractometry data, relation (2) should be written for a number of specific scattering angles $\theta_1, \theta_2, \ldots$. Then we obtain a linear system of equations relating the parameters $F(\theta_1), F(\theta_2), \ldots$ and $p_1, p_2, \ldots$. Solving this system, we can define a set of parameters $p_1, p_2, \ldots$, i.e., to reconstruct the distribution $p_j(R_j)$.

3. Experimental

3.1. Preparation of blood samples

We examined three blood samples of healthy donors (males aged 20 to 23). To prepare a suspension, blood was separated from plasma with phosphate buffered saline. Washed red blood cells were obtained by centrifugation and removal of supernatant liquid. This procedure was carried out two–three times and led to the purification of red blood cells from plasma proteins. As a result, erythrocyte aggregation (bonding) decreased. The resulting solution in an amount of 10 μL was placed between a cover slip and a slide, separated by approximately 100 μm. The erythrocyte concentration in the solution should be sufficient to observe the diffraction pattern; however, a too large cell concentration may lead to their bonding and formation of complex structures that are similar to crystalline. This process can cause changes in the intensity distribution of the diffraction pattern [5]. The appearance of a wet smear of blood under a microscope is shown in Fig. 1a.

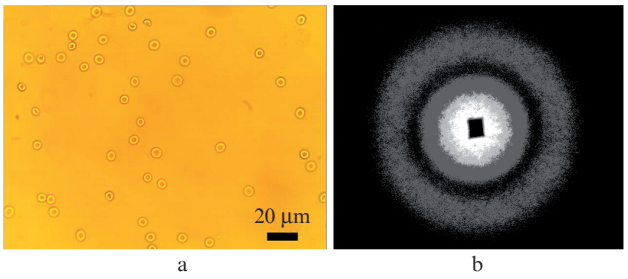

Figure 1. (a) Appearance of a wet blood smear under a microscope and (b) diffraction pattern occurring in the scattering of light by the blood smear.

3.2. Experimental setup

Our experimental setup comprises a helium–neon laser, a polarisation attenuator, a system for generating a light beam, a screen for observing the diffraction pattern, a camera and a computer. In this paper we used a Hamamatsu ORCA Flash 4.0 technical camera; a translucent screen was a sheet of white paper. The scheme of the setup is shown in Fig. 2.

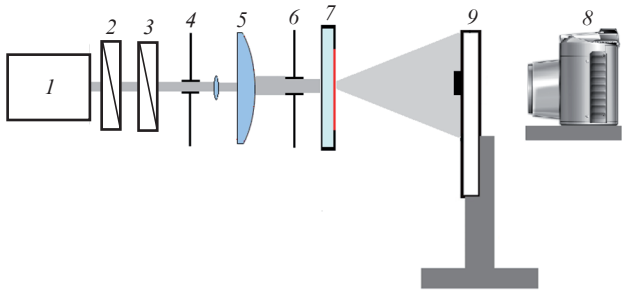

Figure 2. Experimental setup:
(*1*) He–Ne laser; (*2*, *3*) polarisers; (*4*, *6*) apertures; (*5*) lens system; (*7*) blood smear; (*8*) camera; (*9*) translucent screen with a laser-beam absorbing plate.

The power of the 633-nm helium–neon laser was adjusted by a system of crossed polarisers. The laser light intensity should be attenuated so that to ensure that the recorded diffraction pattern does not extend beyond the dynamic range of the CCD camera. The laser power up to the system of polarisers was 1 mW. Due to the chaotic arrangement of red blood cells on the smear surface, the diffraction pattern was characterised by speckle noise. For the speckles (spots) to be small compared to the size of the diffraction pattern, we increased the diameter of the laser beam with a telescopic lens system by approximately two times (up to 2 mm). Lenses and polarisers have dust and scratches, on which the laser beam is diffracted and partially dispersed. Thus, there arises a parasitic interference pattern in the form of contrasting concentric rings violating the uniformity of illumination. To eliminate this effect, we used spatial filters, i.e., apertures (*4*) and (*6*). After scattering on a blood smear (*7*), light was incident on the observation screen and photographed.

To prevent incidence of non-scattered laser light on the camera matrix, we fixed on a paper screen a laser-beam absorbing square plate with a side of 5 mm. The plate was mounted on that part of the paper screen onto which the laser beam fell in the absence of the smear. The sensor of the camera had the following characteristics: 13.3 × 13.3-mm black-and-white CMOS sensor with a resolution of 2048 × 2048 pixels and a 16-bit ADC. Air cooling made it possible to lower the sensor temperature down to –10 °C, which reduced the noise and thus increased the dynamic range of measurements. The camera was controlled by a computer, which also allowed processing of the registered image.

3.3. Diffraction of the laser beam on a reference object

To demonstrate the ability to obtain correct information about the intensity distribution in the measured scattering pattern, we performed an experiment with a reference object, in the form of a thin slit, on the assembled setup. Figure 3 shows the measured light intensity distribution in the diffraction pattern. Diffraction of a plane light wave at the slit of width d is described by the formula [19]

$$\frac{I}{I_0} = \left[\frac{\lambda z}{\pi dx}\sin\left(\frac{\pi dx}{\lambda z}\right)\right]^2, \tag{3}$$

where x is the coordinate on the observation screen, and z is the distance from the screen with the slit to the observation screen. The theoretical curve plotted by formula (3) at d = 128 μm is shown in Fig. 3. Measuring the slit width with a microscope yielded d = 127 μm, which is consistent (within the error) with the data of laser diffractometry. The results presented in Fig. 3 lead to the conclusion that the photometry of the diffraction pattern is conducted properly in a sufficiently wide range of light intensities.

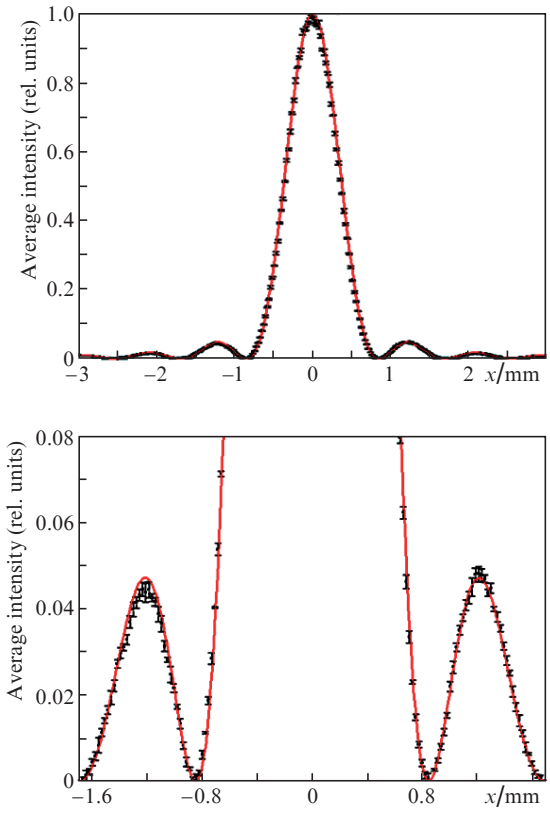

Figure 3. Light intensity distribution in the diffraction pattern obtained on the slit. Points show the photometry data of the diffraction pattern obtained by the camera; the solid curve is constructed using formula (3).

4. Experimental results and their processing

4.1. Scattering of light on a blood smear

The diffraction pattern obtained for a laser beam scattered on a blood smear is shown in Fig. 1b. The blood smear was fixed on a vertical translator (see Fig. 2). To reduce the influence of the speckles, we displaced several times the smear by 1 mm during shooting in a plane perpendicular to the plane of the figure. To reduce the influence of background light, images were taken in a darkened room.

The measured intensity distributions were averaged over 20 frames in order to suppress the speckle noise of the diffraction pattern. In addition, after each measurement we took images with the laser turned off. Background levels assessed with the help of such images were subtracted from the data containing information about the intensity distribution in the diffraction pattern. This made it possible to reduce the influence of noise components and eliminate the background light. The described processing procedures were implemented by using the MATLAB software package and LabVIEW graphical development environment. Distributions obtained with the blood smears were smoothed by a running average. The smoothing window was chosen so that the depth of the dip of the first diffraction minimum remained the same. The intensity distribution resulting from the processing of recorded images is presented in Fig. 4.

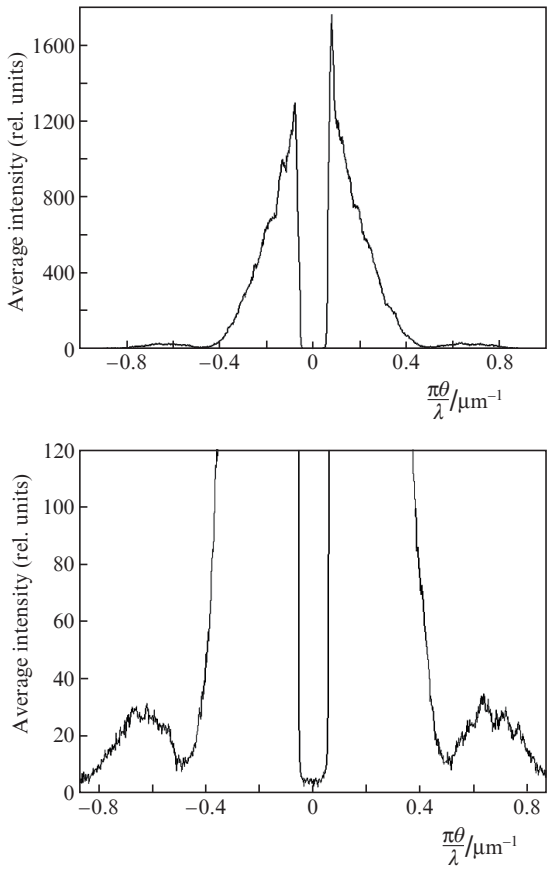

Figure 4. Angular distribution of the light intensity in the diffraction pattern obtained from a wet blood smear.

4.2. Analysis of experimental data using a simplified model of a red blood cell

In this section we analyse the obtained data by using a simplified model of a red blood cell – a flat disc model, in which the light intensity distribution in the diffraction pattern is described by formula (2). The parameters β and Φ, as well as the distribution $p_j(R_j)$ in this formula are selected in such a way as to ensure the best fit of the theoretical intensity distribution with the experimental data shown in Fig. 4. The result of the approximation is shown in Fig. 5. One can see that the experimental and theoretical distributions are in good agreement with each other. Using the thus found red cell size distribution $p_j(R_j)$, we calculated the average radius $\bar{R}$ of a red blood cell, and the variation of red blood cells in size δ_R for this blood sample. Then, the same parameters were measured with a microscope. These procedures we repeated for the other two blood samples. The data obtained are presented in Table 1. Here are the results of measurements of the average radius of erythrocytes and the scatter of red blood cells in size, made by diffractometry and microscopy methods. It can be seen that the error in the measurement of these parameters by the diffractometry method is less than 10%. This allows us to draw a conclusion that our theoretical model is adequate and that the laser diffractometry method can be used to measure parameters of the red cell size distribution.

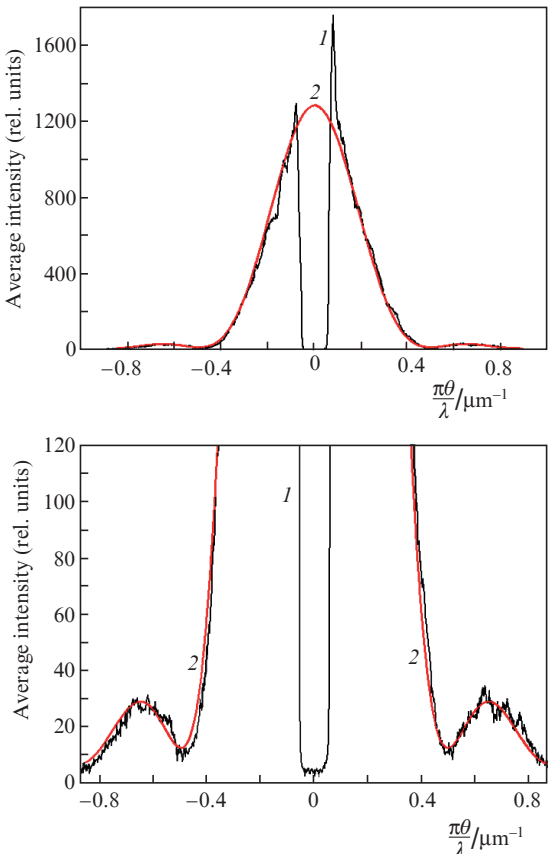

Figure 5. (*1*) Experimental and (*2*) theoretical distributions of the light intensity in the diffraction pattern obtained in the scattering of a laser beam by a wet blood smear. The theoretical distribution is constructed using formula (2).

Table 1. Parameters of red cell size distribution determined by the methods of diffractometry and microscopy.

Donor	Method	
	Diffractometry	Microscopy
1	$\bar{R} = 3.9 \pm 0.4$ μm	$\bar{R} = 3.9 \pm 0.4$ μm
	$\delta_R = 7.0 \pm 0.8\%$	$\delta_R = 7.2 \pm 0.8\%$
2	$\bar{R} = 4.2 \pm 0.5$ μm	$\bar{R} = 3.9 \pm 0.4$ μm
	$\delta_R = 7.8 \pm 0.9\%$	$\delta_R = 8.5 \pm 0.9\%$
3	$\bar{R} = 4.0 \pm 0.4$ μm	$\bar{R} = 3.9 \pm 0.4$ μm
	$\delta_R = 8.6 \pm 0.9\%$	$\delta_R = 9.5 \pm 0.9\%$

4.3. Solution of the inverse scattering problem with allowance for the real shape of the erythrocyte

This section provides a general method for solving the inverse scattering problem and analyses the experimental data on laser diffractometry of a wet blood smear, taking into account the real shape of red blood cells. The angular distribution of the scattered light intensity, observed in the far-field diffraction region, is denoted by $\tilde{I}(\theta)$. In a real experiment, it is determined with some uncertainty, and we can assume to know the norm

$$\int_{\theta_1}^{\theta_2} |\tilde{I}(\theta) - \bar{I}(\theta)|^2 \mathrm{d}\theta = \left\| \tilde{I} - \bar{I} \right\|^2 = \delta^2$$

of the difference between the experimentally measured intensity distribution and the distribution corresponding to the theoretical model $\bar{I}(\theta)$ in the class of function $L_2[\theta_1, \theta_2]$. This class includes all continuous functions and discontinuous functions in a finite number of points. Here, $[\theta_1, \theta_2]$ are the boundaries of the angular range in which diffraction occurs.

Let $w(R)$ be the probability density function for the radius of a red blood cell, and $I(R,\theta)$ is the intensity of light scattered by a red blood cell of radius R in the direction θ. Then, the function $w(R)$ can be considered as a solution of the integral equation

$$N \int_{R_1}^{R_2} I(R,\theta) w(R) \mathrm{d}R = \tilde{I}(\theta), \tag{4}$$

where N is the number of red blood cells irradiated by the laser; and R_1 and R_2 are the minimal and maximum radii of red blood cells in the ensemble, respectively. The type of the function $I(R,\theta)$ depends on the adopted approximations regarding the shape of the erythrocyte. Here we use a more accurate model of a red blood cell – a biconcave disc model. The thickness of the red blood cell in the centre of the disc will be considered equal to $2R/7.5$, and on the periphery of the cell – $4R/7.5$ at the disc radius R (in μm). We will calculate numerically the function $I(R,\theta)$, using the discrete dipole approximation and ADDA programme described in [22].

As shown in [23], the stability of the solution of equation (4) will increase significantly if we multiply both sides of (4) by θ^3, multiply and divide the integrand by R and seek the unknown function $Rw(R)$. Thus, below, instead of equation (4) we will have in mind an equivalent, but with better properties, equation

$$N \int_{R_1}^{R_2} \left[\frac{\theta^3 I(R,\theta)}{R} \right] [Rw(R)] \mathrm{d}R = \theta^3 \tilde{I}(\theta). \tag{5}$$

It is known (see, for example, [23]) that problem (4) is incorrectly set in the sense that although it has a unique solution, it is, however, unstable. The integral operator in the left-hand side of (4), by virtue of the continuity of the kernel function $I(R,\theta)$, is linear and completely continuous. This means that Tikhonov's regularisation method (see, for example, [24]) can be applied to it. Consider the Tikhonov functional

$$M(w) = \left\| Aw - \tilde{I} \right\|^2 + \alpha \|w\|^2, \tag{6}$$

where A is the integral operator in the left-hand side of equation (4); the first norm is taken in the class of functions $L_2[\theta_1, \theta_2]$, and the second – in a narrower class of functions $W_2^1(R_1, R_2]$, to which only continuous functions actually belong. The regularisation parameter α is determined by the trial-and-error method. To improve the accuracy of data recovery, we took into account the following *a priori* information about the function $w(R)$: smoothness of the function $[w(R) \in W_2^1[(R_1, R_2]]$, finiteness of the range of variation of the particle radii ($R_1 \leqslant R \leqslant R_2$), and non-negativity of the function $[w(R) \geqslant 0]$. For a correct account of the last two conditions, functional (6) was minimised in accordance with the following iterative procedure [25]:

$$w_{k+1} = w_k + \beta A^{\mathrm{T}} \tilde{I} - \beta (A^{\mathrm{T}} A + \alpha H) w_k, \tag{7}$$

where β is the real sufficiently small constant, which is determined by the condition $0 < \beta < 2/\lambda_{\max}$; and $\lambda_{\max}$ is the maximum eigenvalue of the matrix $A^{\mathrm{T}}A + \alpha H$. The matrix H is determined by the partition step of the interval $[R_1, R_2]$. The explicit form of this matrix is given in [24] (Chapter 1, Section 5). If in the right-hand side of (7) $w_{k+1}(R_i) < 0$, then we assumed that $H = 0$. In addition, for any value of k, we assumed that $w_{k+1}(R_1) = w_{k+1}(R_2) = 0$. In our calculations, this method led to correct results already at a sufficiently small ($\sim$10) number of iterations, although formally in the numerical experiment, convergence is achieved only when the number of iterations is equal to $\sim 10^4$. For all the calculations, from the experimental data on intensity $\tilde{I}(\theta)$ we selected an interval $[\theta_1, \theta_2]$ from 2 to 10° with a discrete uniform partitioning into 60 points. The interval $[R_1, R_2]$ was set equal to 2–7 μm with a partitioning into 200 points, which gives a sufficiently good approximation of the integral in the left-hand side of (4) by the finite partial sum. The thus obtained distribution $w(R)$ for one of the blood samples is shown by the solid curve in Fig. 6. The dashed curve shows the red cell size distribution determined with a microscope. Note the similarity of the obtained distributions. In particular, it is estimated that the average diameters of the erythrocytes in this blood sample, obtained by diffractometry and microscopy methods, differ by less than 1%, while the estimates of the erythrocyte scatter in size differ by about 20%.

5. Conclusions

We have developed an experimental setup for laser diffractometry of a blood smear and for measurements of red cell size distribution. Experiments with a reference object (narrow slit) have shown that this setup allows photometry of diffraction patterns in a fairly wide range of light intensities. For diffractometry we have used a wet blood smear, which is actually a thin layer of a suspension of red blood cells. For the interpretation of the experimental data we applied the theoretical model in which red blood cells are presented by flat or

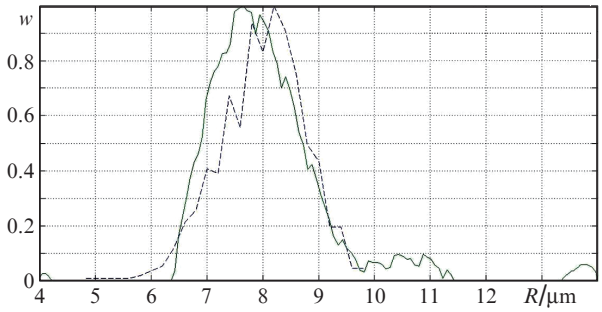

Figure 6. Red cell size distributions determined by (solid curve) diffractometry and (dashed curve) microscopy for a wet smear of blood. In measurements by both methods, erythrocyte ensembles containing approximately 1000 cells have been processed. In the theoretical model, the real shape of the red blood cell (a biconcave disc) has been taken into account. Scattering of light on a red blood cell is calculated in the discrete dipole approximation using the ADDA programme, and the inverse scattering problem is solved using Tikhonov's regularisation method.

biconcave discs. Using a simplified model of a red blood cell (flat disc model), we have solved the direct problem of scattering and calculated the light intensity distribution in the diffraction pattern, based on the known size distribution of erythrocytes. The calculation has shown good agreement between experimental and theoretical distributions. This leads to the conclusion about the adequacy of our theoretical model. Using a more accurate model of the red blood cell (biconcave disc model), we have solved the inverse scattering problem and reconstructed the red cell size distribution in the blood sample. The thus obtained distribution has proven to be very similar to the distribution measured using a microscope. In particular, the average diameter of an erythrocyte is determined with an error of less than 1%, and the scatter of erythrocytes in size – with an error of about 20%. Thus, laser diffractometry allows the red cell size distribution to be measured in suspensions of oriented erythrocytes.

Acknowledgements. The authors are grateful to I.V. Golovnin for useful discussions and valuable advice. This work was supported by the Russian Foundation for Basic Research (Grant Nos 13-02-01372 and 15-32-51068) and the UMNIK grant ('Development of an innovative laser analyser of red blood cells' project).

References

1. Kushang V. P., Luigi F., Ershler W.B., Longo D.L., Guralnik J.M. *Arch. Intern. Med.*, **169** (5), 515 (2009).
2. Canham P.B., Burton A.C. *Circulation Research*, **22**, 405 (1968); DOI: 10.1161/01.RES.22.3.405.
3. http://www.coultercounter.co.uk/.
4. Kozinets G.I., Pogorelov V.M., Shmarov D.A., Boev S.F., Sazonov V.V. *Kletki krovi – sovremennye tekhnologii ikh analiza* (Blood Cells – Advanced Techniques of Their Analysis) (Moscow: Triada-Farm, 2002).
5. Krakau C.E.T. *Biophys. J.*, **6**, 801 (1966).
6. Aksenov E.T., Mokrova D.V. *Pis'ma Zh. Tekh. Fiz.*, **34** (20), 38 (2008).
7. Yang Y., Zhang Z., Yang X., Yeo J.H., Jiang L.J., Jiang D. *J. Biomed. Opt.*, **9** (5), 995 (2004).
8. Yao C., Li Z., Zhang Z. *Chin. Opt. Lett.*, **2** (6), 343 (2004).
9. Nikitin S.Yu., Priezzhev A.V., Lugovtsov A.E. In: *Advanced Optical Flow Cytometry: Methods and Disease Diagnoses*. Ed. by V.V. Tuchin (Weinheim: Wiley-VCH Verlag GmbH & Co., 2011) p. 133.
10. Nikitin S.Yu., Lugovtsov A.E., Priezzhev A.V., Ustinov V.D. *Kvantovaya Elektron.*, **41** (9), 843 (2011) [*Quantum Electron.*, **41** (9), 843 (2011)].
11. Yurkin M.A., Semyanov K.A., Tarasov P.A., Chernyshev A.V., Hoekstra A.G., Maltsev V.P. *Appl. Opt.*, **44** (25), 5249 (2005).
12. Constantinides G.N., Gintides D., Kattis S.E., Kiriaki K., Paraskeva C.A., Payatakes A.C., Polyzos D., Tsinopoulos S.V., Yannopoulos S.N. *Appl. Opt.*, **37** (31), 7310 (1998).
13. Ergul O., Arslan-Ergul A., Gurel L. *J. Biomed. Opt.*, **15** (4), 1 (2010).
14. Lim J., Ding H., Mir M., Zhu R., Tangella K., Popescu G. *Biomed. Opt. Express*, **2** (10), 2784 (2011).
15. Nikitin S.Yu., Priezzhev A.V., Lugovtsov A.E. *J. Quant. Spectrosc. Radiat. Transfer*, **121**, 1 (2013).
16. Van de Hulst H.C. *Light Scattering by Small Particles* (New York: John Wiley & Sons, 1980; Moscow: IL, 1961).
17. Nikitin S.Yu., Lugovtsov A.E., Priezzhev A.V. *Kvantovaya Elektron.*, **40** (12), 1074 (2010) [*Quantum Electron.*, **40** (12), 1074 (2010)].
18. Born M., Wolf E. *Principles of Optics* (Oxford: Pergamon Press, 1964; Moscow: Nauka, 1973).
19. Akhmanov S.A., Nikitin S.Yu. *Physical Optics* (Oxford: Claredon press, 1997; Moscow: Nauka, 2004).
20. Bessmel'tsev S.S., Lendyaev A.V., Tarlykov V.A. In: *Opticheskie lazernye tekhnologii* (Optical Laser Technologies) (Saint Petersburg: SPbGU ITMO, 2001) p. 120.
21. Magurin V.G., Tarlykov V.A. *Kogerentnaya Optika* (Coherent Optics) (SPb.: Izd. SPbGU ITMO, 2006).
22. Yurkin M.A., Hoekstra A.G. *J. Quant. Spectrosc. Radiat. Transfer*, **112** (13), 2234 (2011).
23. Riley J.B., Agrawal Y.C. *Appl. Opt.*, **30** (33), 4800 (1991).
24. Tikhonov A.N., Goncharsky A.V., Stepanov V.V., Yagola A.G. *Numerical Methods for the Solution of Ill-Posed Problems* (Boston, Mass.: Kluwer Academic, 1995; Moscow: Nauka, 1990).
25. Vasil'ev F.P. *Metody optimizatsii* (Optimisation Methods) (Moscow: Factorial Press, 2002).